Size-Differentiated Lateral Migration of Bubbles in Couette Flow of Two-Dimensional Foam

Hadi Mohammadigoushki[1] and James J. Feng[1,2]

[1]Department of Chemical and Biological Engineering, University of British Columbia, Vancouver, British Columbia V6T 1Z3, Canada
[2]Department of Mathematics, University of British Columbia, Vancouver, British Columbia V6T 1Z2, Canada

(Received 15 May 2012; published 21 August 2012)

We report experiments on lateral migration of bubbles in a two-dimensional foam sheared in a narrow-gap Couette device. A larger bubble in an otherwise monodisperse bubble raft migrates toward the center of the gap as long as the bubble size ratio and the shear rate are each above a threshold. The migration speed is roughly two orders of magnitude higher than that of a single bubble, and increases with the shear rate and the size ratio. The bubble also deforms much more than an isolated one at the same shear rate. Modifying the Chan–Leal solution for the migration of a single submerged bubble or drop, we derive a formula that successfully predicts all the migration trajectories recorded in the experiment. The threshold for migration corresponds to the wall repulsion force overcoming the capillary force in the two-dimensional foam. The size-differentiated bubble migration provides an explanation for previously observed size segregation in sheared three-dimensional polydisperse foams.

DOI: 10.1103/PhysRevLett.109.084502 PACS numbers: 47.55.D−, 47.55.dd, 47.57.Bc

Foam is often studied as a model soft matter, as it exhibits interesting mechanical behaviors such as jamming and yielding [1,2]. Its rheology and hydrodynamics are intimately coupled to its microstructure, i.e., the shape and spatial organization of the bubbles [3,4]. A particularly intriguing phenomenon is size-based segregation of bubbles in a polydisperse foam [5]. After shearing between rotating parallel plates, smaller bubbles appear predominantly near the top and bottom plates, while the larger ones are in the middle. The cause is unclear, but one possibility is that the bubbles have migrated across streamlines based on their size. In a more recent experiment on a two-dimensional (2D) foam under oscillatory shear [6], a bubble larger than its monodisperse neighbors migrates toward one of the four borders confining the foam. This seems to contradict the observations of Ref. [5]. More curiously, the migration does not distinguish between the flow direction and the direction of the velocity gradient. These two studies hint at some rule governing lateral migration of bubbles in sheared foam, but little is known at present.

In contrast, the lateral migration of particles and droplets suspended in a liquid medium has been extensively studied in the past (for example see Refs. [7–10]). A solid spherical particle in a Stokes flow cannot migrate because the linear system is time reversible. A droplet deforms under shear, and this introduces a nonlinearity into the problem and enables lateral migration. It has been shown that in low-Reynolds-number Couette flows, droplets move away from the walls toward the center of the gap [8,11,12]. This is commonly interpreted as a wall repulsion: the rigid wall produces an asymmetry in the velocity and pressure fields around the drop, resulting in lateral migration force. Naturally, one wonders if the same repulsion operates in sheared foam.

This Letter describes an experimental study of lateral migration of bubbles in a 2D foam sheared steadily in a narrow-gap Couette device. Into a monodisperse bubble raft, we introduce a single bubble of different size and investigate its migration. By correlating the migration speed with the shear rate and the bubble size ratio, we propose a hydrodynamic explanation for the migration based on bubble deformation.

The experiments are carried out in a modified Couette device consisting of a rotating sharp-edged inner disk of radius $R_1 = 9.3$ cm and a stationary outer cylinder of inner radius $R_2 = 10$ cm. Blowing nitrogen bubbles into a surfactant-glycerin solution in water, we are able to produce highly monodisperse bubble rafts that rest on the free surface. The surfactant used is Sunlight dishwashing liquid (Unilever), and the liquid bath is 10 cm deep. The bulk surfactant concentration $c = 5$ wt.% is 100 times the critical micelle concentration. Such a high concentration immobilizes the bubble surface and prevents bubble bursting [13]. The liquid contains 80 wt.% glycerin, and has a viscosity $\mu = 50 \pm 1$ mPa s, density $\rho = 1200$ kg/m^3, and surface tension $\sigma = 25 \pm 2$ mN/m. The area fraction of gas in the foam, or foam quality, is around 85%. More details on the experimental setup and material characterization can be found in our earlier paper on bubble coalescence [13].

To study bubble migration, we insert a "test bubble" of radius R into the bubble raft, R being different from the background bubble radius r, and shear the foam by rotating the inner cylinder. The trajectory of the test bubble is recorded using three cameras from above. The rotational speed of the inner cylinder Ω ranges from 0.05 to 10 rpm. Using the shear rate $\dot{\gamma} = \Omega R_1/d$, $d = R_2 - R_1$ being the gap width, we define a bubble Reynolds number $\mathrm{Re} = \rho\dot{\gamma}R^2/\mu$ and a capillary number $G = \mu\dot{\gamma}R/\sigma$. G falls in the range $5 \times 10^{-5} \leq G \leq 1.7 \times 10^{-2}$, well below the minimum needed for bubble breakup [14]. Indeed, bubble breakup, coalescence, or burst never happened in

our experiment. We will use both Ω and G in presenting the results; they can be converted into each other through $G = \mu R R_1 \Omega/(\sigma d)$.

Before presenting the results, let us exclude two geometric factors from further consideration. First, for a Newtonian fluid, the narrow gap would ensure an essentially linear velocity profile. But a bubble raft tends to be shear thinning and can exhibit a greater shear-rate gradient across the gap [13,15]. Second, at high rotational speeds, centripetal forces tend to induce an inward motion of bubbles [13,16]. Both have been rendered negligible in our experiment by using highly viscous suspending liquids. The large viscosity suppresses the effective "slip" between the bubble raft and the underlying liquid, and ensures a linear bubble velocity profile. Besides, as long as we keep the bubble Reynolds number $\mathrm{Re} < 0.1$, the centripetal force plays no role in the lateral migration. For the current purpose, therefore, the Couette flow amounts to a simple shear between parallel walls.

As a baseline, we first study the migration of a single bubble floating on the free surface. It migrates to the center of the gap from all initial positions. Typical trajectories are shown in Fig. 1. The dimensionless drop position S is scaled by the gap width d, with $S = 0$ at the inner cylinder and 1 at the outer cylinder. The symmetry between the inward and outward trajectories confirms the uniformity of the shear rate across the gap. This migration is reminiscent of that of neutrally buoyant droplets suspended in a liquid medium [8,12]. Thus we have compared the measured trajectories with those predicted by the theory of Chan and Leal [8]. Note that the prerequisites for the perturbation theory, $\mathrm{Re} \approx 0$, $G \ll 1$, and $R \ll d$, are all satisfied by the experiment. In our geometry, the theory predicts a bubble migration velocity at dimensionless position S

$$v_m(S) = \frac{81}{140}\frac{R^2}{d^2}\frac{\sigma G^2}{\mu} f(S), \qquad (1)$$

where $f(S) = S^{-2} - (1-S)^{-2} + 2 - 4S$, and we have put the bubble-to-liquid viscosity ratio to zero in the original Chan-Leal formula. Integrating the above using the experimental parameters produces the trajectories of Fig. 1. The agreement between the measured and predicted trajectories is very close. The formula was derived for a neutrally buoyant drop inside a three-dimensional (3D) fluid while our bubble "floats" on the liquid surface. In reality, surface tension keeps 99% of the bubble volume below the undisturbed free surface, which is consistent with theoretical calculations [17] (Fig. 1 inset). The viscous friction in the thin meniscus atop the bubble may be larger than in a fully 3D geometry. But apparently the left-right asymmetry dominates and the vertical dimension seems to matter little. Thus, the Chan-Leal formula predicts the migration in our geometry with no fitting parameter.

The main result of the experiment is the migration of a larger bubble of radius R in an otherwise monodisperse bubble raft of radius r. Generally the large bubble migrates toward the center of the gap, and the migration speed depends on the size ratio $\kappa = R/r$ and the rotation rate Ω. Figure 2 shows the migration trajectories for several κ and Ω values. During the migration, the large bubble shifts from one row of bubbles to the next, spending a finite time in each. This is indicated by the horizontal bars on some trajectories, forming a staircase pattern. For clarity, the bars are omitted on the other trajectories with only data points plotted at the center of each step.

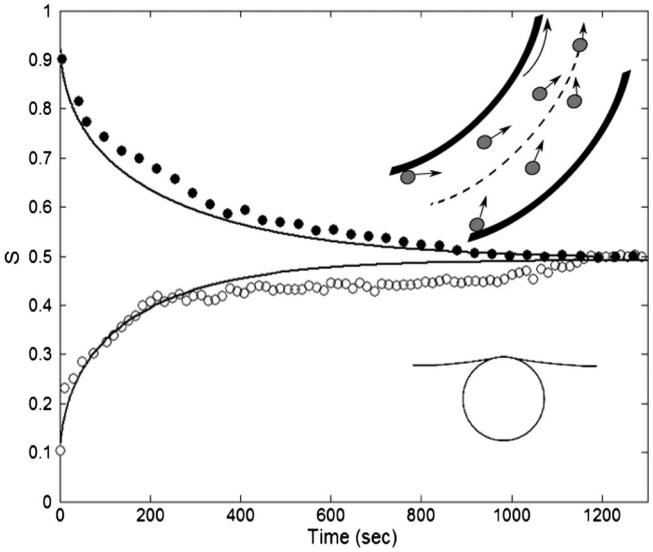

FIG. 1. Migration trajectories of a single bubble ($R = 0.7$ mm) at $\Omega = 7$ rpm. The curves represent the Chan-Leal formula [Eq. (1)]. The top inset illustrates the migration schematically (not to scale) and the bottom one depicts the liquid meniscus above the bubble calculated from the model of Ref. [17].

The following observations can be made. (i) There are a threshold κ_0 for a fixed Ω and a threshold Ω_0 for a fixed κ, below which no migration occurs. For the conditions of Fig. 2(a), κ_0 lies between 1.43 and 1.54. In particular, a bubble smaller than its neighbors, i.e., with $\kappa < 1$, does not migrate at all. In Fig. 2(b), Ω_0 is between 2 and 2.5 rpm. (ii) For sufficiently large Ω and κ, a large bubble migrates all the way to the center ($S = 0.5$). Below these, the bubble may migrate to an intermediate position between the wall and the center. (iii) The migration speed increases with κ and Ω. (iv) The migration is much faster than if a bubble of radius R migrates on a free surface without the bubble raft. This can be seen by comparing Fig. 2 with Fig. 1; the migration time differs by a factor of $O(10^2)$.

All the above observations can be explained by a model based on the deformation of the migrating bubble. Chan and Leal [8] showed that the wall repulsion stems from the left-right asymmetry in the flow around the bubble and the concomitant asymmetric bubble shape. In our experiment, a larger bubble protrudes outside its own row and forces the surrounding bubbles to rearrange as they pass around it [Fig. 3(a)]. Compared to fluid particles in a continuum, the surrounding bubbles have a finite radius r and a capillary pressure inside, and thus are much harder to displace and

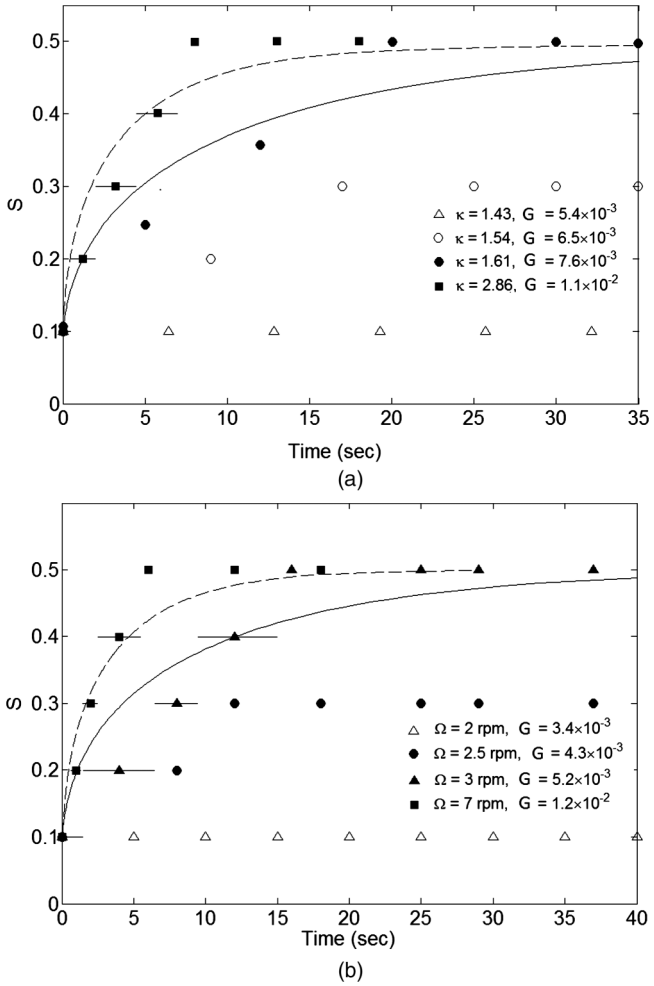

FIG. 2. Bubble migration in a 2D foam. (a) Effect of the bubble size ratio κ at $\Omega = 4$ rpm. The bubble radii are (in mm): $(r, R) = (0.35, 0.5)$ for $\kappa = 1.43$; (0.39, 0.6) for $\kappa = 1.54$; (0.435, 0.7) for $\kappa = 1.61$, and (0.35, 1) for $\kappa = 2.86$. The solid and dashed curves are predictions of Eq. (3) for $\kappa = 1.61$ and 2.86. (b) Effect of the rotational rate Ω for fixed bubble sizes $(r, R) = (0.35, 0.7)$ mm. The curves are predictions of Eq. (3) for $\Omega = 3$ and 7 rpm.

deform. They continuously rub and bump into the sides of the large bubble, imparting a force F_b on it. This force is the counterpart of the liquid pressure and viscous force in the single-bubble scenario, but much larger. A visible consequence of F_b is the pronounced deformation of the large bubble, much more than a single bubble of the same size subject to the same shear rate [Fig. 3(b)]. A less visible one, we surmise, is a strong wall repulsion arising from the asymmetry in F_b from the two sides.

This idea can be made more precise by plotting the bubble deformation as a function of the size ratio κ (Fig. 4). We define a bubble deformation parameter $D = (l - s)/(l + s)$, l and s being the long and short axes of the roughly elliptical deformed bubble, respectively. According to Taylor's celebrated formula [18], a single bubble of negligible internal viscosity in a sheared fluid should have $D = G$. In the bubble raft, we find $D \propto G$ as

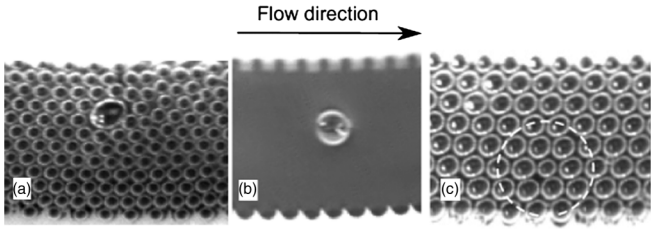

FIG. 3. Bubble deformation in different environments at $\Omega = 7$ rpm. The large bubble ($R = 0.7$ mm) in (a) deforms much more in a foam of smaller bubbles ($r = 0.35$ mm) than alone in (b). (c) A smaller bubble ($R = 0.4$ mm) is shielded by its neighbors ($r = 0.58$ mm).

well, and represent the data by $D/G = g(\kappa) = 2.5\kappa^2 - 7\kappa + 11$. Now we equate the larger deformation in a bubble raft to that of a single bubble at a higher "effective capillary number" G_e:

$$G_e = D = G \cdot g(\kappa). \tag{2}$$

Plugging this into the Chan-Leal formula [Eq. (1)] gives us a modified Chan-Leal formula

$$v_m(S, \kappa) = \frac{81}{140} \frac{R^2}{d^2} \frac{\sigma G^2}{\mu} f(S) g^2(\kappa). \tag{3}$$

After time integration, this formula predicts well all the migration trajectories recorded in our 2D foam, over the entire range of r, R, and Ω values. For clarity, only a few representative curves are plotted in Fig. 2. Note that the $O(10)$ deformation enhancement in Fig. 4 translates to the $O(10^2)$ increase in the migration velocity. The success of Eq. (3) confirms our hypothesis in the preceding paragraph. As a corollary, a bubble of the same size as its neighbors or smaller ($\kappa \leq 1$) does not migrate because it does not jut out

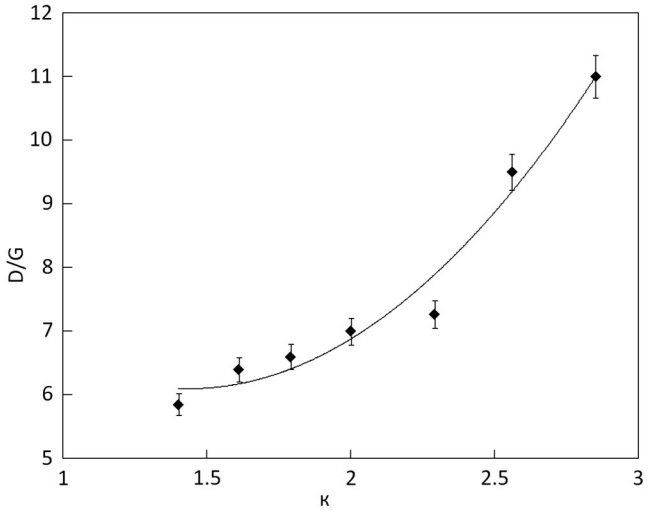

FIG. 4. Deformation parameter of a larger bubble in a 2D foam as a function of the bubble size ratio κ. The error bars indicate the variation among seven shear rates tested, and the curve is a quadratic fit to the data.

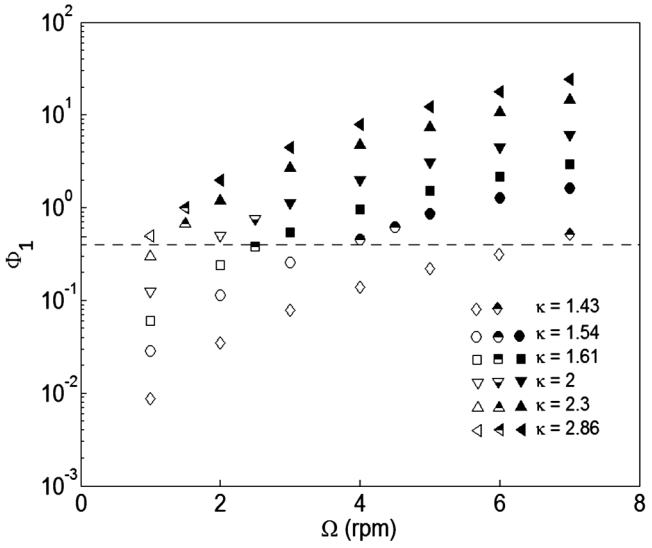

FIG. 5. Threshold for bubble migration. Φ_1, computed from Eq. (4) for the first row of the bubbles next to the wall, is plotted as functions of Ω for various κ values. Hollow, half-filled, and filled symbols indicate no migration, partial migration, and complete migration to the center, respectively. The dashed line is $\Phi_1 = 0.4$.

of its own row [Fig. 3(c)]. Thus, it is not subject to the "bumping force" F_b.

Finally, we examine the thresholds κ_0 and Ω_0 for lateral migration. When a monodisperse 2D foam is sheared, the bubbles typically move in streamwise rows past one another. For a larger bubble (radius R) to migrate laterally, it must squeeze into the next row of bubbles (radius r). The wall repulsion force F_w driving the migration, therefore, must exceed a threshold in order to deform the bubbles of the next row to create the gap. Because these bubbles in turn interact with multiple moving and changing neighbors on the other side, it is difficult to posit a precise force balance from which to calculate the threshold. As an estimation, we take the resistance to migration to be on the same order of magnitude as the capillary force between bubbles in the row: $F_c = (\sigma/r)\pi a^2$, where a is the radius of the thin film between neighboring bubbles in a 2D foam. For the foam quality used here, a shows a normal distribution among the bubble pairs, with a mean of $a = 0.2r$ [13], which will be used below. On the other hand, the wall repulsion can be estimated from the Stokes formula using the migration velocity of Eq. (3): $F_w = 6\pi\mu v_m R$. We use the Stokes formula as opposed to the Hadamard formula because the bubble surface is immobilized by the high surfactant concentration [13]. Now the ratio between these two forces is

$$\Phi = \frac{F_w}{F_c} = \frac{243}{70}\frac{R^3 r}{a^2 d^2} G^2 f g^2. \quad (4)$$

Note that $f(S)$ gives the wall repulsion at position S. In particular, using the largest F_w for the first row next to the wall gives us the ratio Φ_1. We argue that a Φ_1 value of $O(1)$ gives the threshold for lateral migration of the larger bubble.

Figure 5 plots Φ_1 for all the κ and Ω values tested in our experiments. The experimental conditions giving rise to lateral migration are indicated by filled and half-filled symbols, the latter for partial migration to positions between the wall and the center. The nonmigrating conditions are shown by hollow symbols. These two groups are almost perfectly separated by $\Phi_1 = 0.4$, thus validating Eq. (4) as an approximation for the threshold. For lower Ω, three data points fall on the wrong side of the line; the experiment may have been more susceptible to external disturbances in these cases. Note that the thresholds reflect the graininess of the bubble raft and have no counterpart in the Chan-Leal theory.

To conclude, we have discovered a size-differentiated lateral migration in sheared 2D foam, and constructed a model based on the Chan-Leal theory to account for the observations. The mechanism offers a potential explanation for the size-based segregation in sheared 3D polydisperse foam [5].

We thank G. M. Homsy for helpful discussions and G. Ghigliotti for critiquing the manuscript and making insightful suggestions. The study was supported by NSERC, the Canada Research Chair program, and the Canada Foundation for Innovation.

[1] J. Goyon, A. Colin, G. Ovarlez, A. Ajdari, and L. Bocquet, Nature (London) **454**, 84 (2008).
[2] G. Katgert, B. P. Tiche, M. E. Mobius, and M. van Hecke, Europhys. Lett. **90**, 54002 (2010).
[3] R. Höhler and S. Cohen-Addad, J. Phys. Condens. Matter **17**, R1041 (2005).
[4] D. Weaire, Curr. Opin. Colloid Interface Sci. **13**, 171 (2008).
[5] B. Herzhaft, J. Colloid Interface Sci. **247**, 412 (2002).
[6] C. Quilliet, M. Idiart, B. Dollet, L. Berthier, and A. Yekini, Colloids Surf. A **263**, 95 (2005).
[7] C. E. Chaffey, H. Brenner, and S. G. Mason, Rheol. Acta **4**, 64 (1965).
[8] P. C. H. Chan and L. G. Leal, J. Fluid Mech. **92**, 131 (1979).
[9] L. G. Leal, Annu. Rev. Fluid Mech. **12**, 435 (1980).
[10] S. D. Hudson, Phys. Fluids **15**, 1106 (2003).
[11] A. Karnis and S. G. Mason, J. Colloid Interface Sci. **24**, 164 (1967).
[12] K. G. Hollingsworth and M. L. Johns, J. Colloid Interface Sci. **296**, 700 (2006).
[13] H. Mohammadigoushki, G. Ghigliotti, and J. J. Feng, Phys. Rev. E **85**, 066301 (2012).
[14] K. Golemanov, S. Tcholakova, N. D. Denkov, K. P. Ananthapadmanabhan, and A. Lips, Phys. Rev. E **78**, 051405 (2008).
[15] J. Lauridsen, M. Twardos, and M. Dennin, Phys. Rev. Lett. **89**, 098303 (2002).
[16] E. Climent, M. Simonnet, and J. Magnaudet, Phys. Fluids **19**, 083301 (2007).
[17] R. A. Medrow and B. T. Chao, Phys. Fluids **14**, 459 (1971).
[18] G. I. Taylor, Proc. R. Soc. A **146**, 501 (1934).